ELSEVIER

Biochimica et Biophysica Acta 1327 (1997) 231–241

BIOCHIMICA ET BIOPHYSICA ACTA
BBA

The anion transporter and a 28 kDa protein are selectively photolabeled by *p*-azidobenzylphlorizin under conditions that alter RBC morphology, flexibility, and volume

Daniel M. Hoefner [a,*], Michael E. Blank [b], Donald F. Diedrich [a,c]

[a] *Graduate Center for Toxicology, University of Kentucky, Lexington, Kentucky 40536, USA*
[b] *University of Hamburg, University Hospital Eppendorf, Department of Veg. Physiology, Martinistrasse 52, 20251 Hamburg, Germany*
[c] *Department of Pharmacology, University of Kentucky, Lexington, Kentucky 40536, USA*

Received 11 December 1996; accepted 28 February 1997

Abstract

Tritiated *p*-azidobenzylphlorizin (*p*-AzBPhz) was photoactivated in the presence of red blood cells under conditions previously found to alter morphology, flexibility and volume. When less than 0.25 million molecules were *added* per cell, only a 28 kDa peptide was photolabeled; at 1–2 million molecules added, band 3 also incorporated significant radioactivity. When using leaky ghosts, other proteins became labeled, including those limited to the cytoplasm. Protein *N*-deglycosylation caused a shift of radiolabeled band 3 to higher R_f values on SDS-PAGE gels but not for the 28 kDa band; the latter was, however, susceptible to enzymatic digestion by NANase (*N*-acetylneuraminidase) III but not by NANase II. Inhibition of photoincorporation into both receptors by unlabeled *p*-AzBPhz was dose-dependent. Mercuric chloride and *p*-CMBS selectively blocked 28 kDa peptide labeling. DIDS partially blocked at band 3; after ~15% inhibition, greater DIDS concentrations caused *increased* incorporation into the 28 kDa peptide. These results, and a temperature-dependent labeling pattern, suggest that: (i) cellular changes occur when *p*-AzBPhz binds to the exofacial sides of the anion transporter and 28 kDa peptide; (ii) these proteins may be physically associated in the native membrane; (iii) they mediate ligand-induced changes in morphology, flexibility, and volume. © 1997 Elsevier Science B.V.

Keywords: Photoaffinity probe; Erythrocyte membrane; Cytoskeleton; Band 3; DIDS; *p*-AzBPhz

1. Introduction

The red blood cell (RBC) is required to deform many thousand times as it maneuvers through the microcirculation and is subjected to continual flow-generated shear forces. The cell must therefore possess some inherent mechanism that permits it to rapidly and reversibly modify its discoid shape. The normal biconcave form of the unstressed red cell is maintained by a dense two-dimensional cytoskeleton – primarily a hexacentric lattice of spectrin, accompanied by actin and band 4.1. This support scaffold is anchored to the membrane bilayer through attachments with the cytoplasmic portions of intrinsic proteins, e.g., the anion exchanger (band 3) and the glycophorins, C and D. A growing number of pro-

* Corresponding author. Mayo Clinic, Clinical Biochemistry, 200 First Street S.W., Rochester, Minnesota 55905, USA. Fax: (507)-284-9758; E-mail: hoefner.daniel@mayo.edu

PII S0005-2736(97)00068-0

teins have been described [1–5] as necessary accessories for the organization and regulation of this membrane-cytoskeletal complex.

We have previously shown that at the same low μM concentrations in which *p*-azidobenzylphlorizin (hereafter, *p*-AzBPhz or, simply, azide) inhibits the RBC anion transporter, water influx occurs as well as flexibility and morphology changes that reflect cytoskeletal alterations [6,7]. To more directly identify the membrane proteins which mediate these phenomena, intact cells were photolabeled with the tritiated azide under comparable conditions. A modified Laemmli [8] polyacrylamide gel electrophoresis method was then used to separate and identify the membrane-associated proteins. Band 3 and a 28 kDa peptide were found to be selectively labeled in a dose-dependent manner; DIDS limited the photolabeling of the anion exchanger and covalent binding to the 28 kDa protein was selectively blocked by low levels of $HgCl_2$ and *p*-(chloromercuri)benzene sulfonate (*p*-CMBS), both recognized as potent inhibitors of water flux across the red blood cell [9–11]. Treatment of the photolabeled proteins with glycosidases, followed by polyacrylamide gel electrophoresis, was used to determine their glycoprotein nature. The data presented here are concordant with our hypothesis that improved rheology and a small increase in water content in the red blood cell follow from a selective interaction of *p*-AzBPhz with the anion exchanger and a 28 kDa peptide.

2. Materials and methods

2.1. Reagents and buffers

p-Azidobenzylphlorizin was synthesized from the corresponding amine as previously described [12]. The specific activity of the [^{3}H]*p*-AzBPhz was 13.4 Ci/mmol, with the tritium incorporated into the A-ring. DIDS was supplied by Molecular Probes, Inc. (Eugene, OR, USA). $HgCl_2$ and *p*-CMBS were from Sigma Chemical Co. Deglycosylation enzymes were supplied by Glyko, Inc. (Novato, CA, USA). Buffers were made with reagent-grade chemicals: glycylglycine buffered saline (GGBS) was 10 mM glycylglycine.HCl, pH adjusted to 7.40 (at 26°C) with NaOH and osmolarity to 289 mOsm/kg with NaCl. Buffers were filtered through 0.2 μm filters (Amicon, Lexington, MA, USA) prior to use.

2.2. Erythrocyte labeling studies

Blood was drawn after informed consent from hematologically normal volunteers into Vacutainer K_3 EDTA tubes. Cells were centrifuged for 5 min at $1200 \times g$; plasma and buffy coat were replaced with GGBS to resuspend the cells. After two additional washes, the hematocrit was adjusted to 5% with GGBS. The recovered plasma was centrifuged at $2700 \times g$ for 20 min to remove platelets and white cells and then diluted with an equal volume of GGBS to wash non-covalently bound ligand from the cells after photolabeling. All buffers used in post-labeling cell isolation procedures contained 0.5 mM PMSF (phenylmethylsulfonyl fluoride) and 1 mM EDTA to inhibit proteases.

Ethanolic solutions of [^{3}H]*p*-AzBPhz in borosilicate glass tubes (the azide, in buffer, sticks avidly to plastic) were rapidly evaporated to dryness in a Jouan centrifugal vacuum concentrator. Washed red cells (500 μl, 5% hematocrit) were then added and incubated for 2 min at RT with gentle mixing. In the inhibition studies, washed cells were exposed to antagonists for 5 min prior to adding them to the [^{3}H]*p*-AzBPhz-containing tubes. After 2 min, the sample was transferred to a porcelain spot dish, slowly stirred with a glass-encased magnetic stir bar, and irradiated using a Schütt Labortechnik 16 W lamp (Heidelberg, Germany) that emitted a narrow UV wavelength of 254 nm. The lamp was adjusted to give an intensity of 1 mW/cm^2; the flash time was 2 min (12 000 ergs/mm^2) at RT unless otherwise noted. After photolysis, a small aliquot was taken to determine radioactivity and 450 μl of the cell suspension was transferred into 1 ml of autologous plasma in GGBS (1:1) in 2 ml plastic microcentrifuge tubes. Cells were pelleted and the supernate, containing unbound ligand and photolytic by-products (primarily the amine), was removed. This was followed by two washes, each with 1.5 ml of plasma-free GGBS. After cooling the packed cells in an ice bath, ghosts were made by adding 1.5 ml of cold 20 mOsm GGBS followed by gentle mixing. After 5 min cold incubation, ghosts were pelleted by centrifugation at 14 000 $\times g$ for 15 min at 4°C. Supernate was removed,

followed by one wash (4°C) with 20 mOsm GGBS, which resulted in pink ghosts.

2.3. Polyacrylamide gel electrophoresis

Protein samples were electrophoresed using a modified Laemmli [8] discontinuous SDS-polyacrylamide gel electrophoresis (disc-SDS-PAGE) system. The stacking gel consisted of 3.1% total acrylamide with the bis fraction (N,N'-methylene-bis-acrylamide) at 2.5% in 0.125 M Tris buffer, pH adjusted to 6.8. The separating gel, usually 7.7% total acrylamide, used a 2.7% fraction of bis and 0.375 M Tris buffer with pH adjusted to 9.0. Both gels contained 0.1% SDS and were polymerized with 0.05% TEMED (v/v) and 0.11% ammonium persulfate (w/v). A Desaga Desaphor VA electrophoresis system (Heidelberg, Germany) was used; both anode and cathode tank buffers contained 0.025 M Tris base, 0.192 M glycine, and 0.1% SDS (pH 8.3). Unless noted otherwise, samples were prepared by heating for 10 min at 75°C in sample buffer containing 0.063 M Tris base, 2% SDS, 5% mercaptoethanol, 10% glycerol, and 0.001% bromphenol blue, pH adjusted to 6.8. To determine whether any covalently bound tritium was liberated from or exchanged between the proteins during the 75°C treatment, samples were also processed by freeze-thaw cycling (10 min cycles at −20°C and 37°C). No difference in the protein labeling pattern could be detected by the two methods, although freeze-thawing did not always yield complete protein solubilization. After constant-voltage electrophoresis at 10–12°C, the gels were fixed in a water/methanol/acetic acid mixture, usually followed by staining with Coomassie R-250. Sigma's silver stain kit was used to stain some of the gels according to the product protocol.

2.4. Fluorography and densitometry

Coomassie stained gels intended for fluorography were treated with NEN's En^{3}Hance (Boston, MA, USA) prior to drying the gel onto filter paper. This fluorographic reagent was chosen to reduce diffusion of Coomassie stain during treatment. Unstained gels were treated with either En^{3}Hance or Amersham's Amplify (Arlington Heights, IL, USA) and the fluorography exposure was performed at −70°C using preflashed (A_{540} = 0.1–0.2 units) Fuji RX or Amersham Hyperfilm-MP. Kodak GBX processing chemicals were used for development.

Densitometric analyses were performed using Biosoft's *Scan Analysis* software (Ferguson, MO, USA) installed on a Macintosh IIci. Images of fluorograms or stained gels were transferred to the computer using a Pulnix CCD video camera (Motion Analysis, Eugene, OR, USA). The accuracy of this method has been shown to agree well with dedicated computer-based densitometric systems [13].

Each lane of the Coomassie stained gels was scanned densitometrically; the values for spectrin and actin were used to normalize the data from the corresponding fluorograms for any minor variation in the amount of protein loaded in the different lanes of the gel.

Tritiated protein molecular weight markers, ranging in size from 14 to 97 kDa, were made by photoaffinity labeling Promega (Madison, WI, USA) protein standards with [^{3}H]*p*-AzBPhz (~1:1 ligand to protein stoichiometry). Residual free ligand was then removed by precipitating the labeled proteins with ethanol. Remaining unbound ligand was eluted from the polyacrylamide gel during the processes of fixing, staining, and/or fluorography enhancement.

2.5. Protein purification

In some studies, purified radioactively labeled membrane proteins were isolated for enzymatic deglycosylation or for use as standards. Intact red cells were photolabeled and their ghost proteins were electrophoresed as described. After establishing the position of the two labeled proteins relative to colored molecular weight markers (Sigma Chemical Co.) in an adjacent lane, the appropriate gel area was excised for protein elution. The excised sections of gel corresponded to a 26–31 kDa range for the 28 kDa peptide and 88–108 kDa for band 3. The Isco electrodialysis procedure, as described by Bhown [14], was used to isolate the labeled band 3 and 28 kDa proteins.

2.6. Gel slice quantitation

Individual lanes from some polyacrylamide gels were analyzed by scintillation counting to monitor protein labeling patterns. The gel was aligned on a template and 3.5 mm wide strips cut from the center

of selected lanes were stored at −70°C until sliced. A Holzel gel slicer (Dorfen, Germany) was used to cut a semi-thawed gel strip into uniform 1 mm segments; each piece was then transferred to a scintillation vial and eluted into an aqueous dilution of NEN Solvable (Boston, MA, USA), followed by the addition of NEN Aquasol for scintillation counting as per manufacturers directions.

2.7. Protein deglycosylation

To characterize the linkage of any (oligo)saccharides associated with the proteins of interest, intact RBCs, ghosts, as well as the isolated photolabeled proteins, were subjected to four of Glyko's recombinant glycosidases: (i) *O*-glycosidase DS, which cleaves Ser/Thr-linked Gal(α1,3)GalNAc(β1), was used at 2 mU per assay; (ii) NANase III, specific for β2-3,6,8-linked *N*-acetylneuraminic acid, was used at 3.35 mU; (iii) PNGase F (at 5 mU) releases asparagine (Asn)-linked oligosaccharides; and (iv) NANase II (10 mU), which is specific for β2-3,6-linked *N*-acetylneuraminic acid, was used prior to digestion with *O*-glycosidase DS. Bovine fetuin was included in the assays to assess the quality and specificity of the reaction.

Protein substrate per assay was approximately 250 μg for RBCs, 25 μg for ghosts, 10 μg for band 3, and 1 μg for the 28 kDa peptide. Incubation of the control, NANase III-, and PNGase F-treated samples was at 37°C under gentle shaking for 3.25–11.5 h, 3.25–4.25 h, and 6.5–11.5 h, respectively. Combined hydrolysis with NANase II plus *O*-glycosidase or with NANase II, *O*-glycosidase plus PNGase F, were performed by consecutive incubations with NANase II (1.2–2.3 h), *O*-glycosidase (2.6–9.8 h), and PNGase F (6.5–9.8 h). Enzyme-treated proteins were electrophoresed as described and patterns of Coomassie stain and fluorography were analyzed densitometrically.

3. Results

3.1. Preferential photolabeling of band 3 and 28 kDa peptide

Due to the high degree of quenching by hemoglobin, the percentage covalent incorporation of ligand into intact RBCs was much less than into ghosts. However, both faces of ghost membranes were accessible to the azide and proteins known to be restricted to the cell interior (e.g., spectrin, actin) also became photolabeled – the event was enhanced if leaky ghosts were used. Labeling of these cytoplasmic proteins was not detectable as long as the RBCs remained intact. Photolytic radioactivity incorporation into membrane components was light dose-dependent. At 1 mW/cm^2, barely detectable protein breakdown occurred if flash times were extended beyond 4 min (as determined by densitometry of Coomassie stained gels, data not shown). Therefore, a 2 min flash time was selected which led to covalent incorporation into the red cell membrane of about 3–5% of the added ligand, as determined by scintillation counting.

Fig. 1 displays the SDS-PAGE pattern of the protein MW standards and the photolabeled membrane proteins using intact cells obtained from three different blood donors and the radioactive azide at 1 μM. This three-panel composite compares identical, four-lane sections cut from a single gel, stained with Coomassie (lanes 1–4) and Silver (lanes 9–12), with a replicate section developed as a fluorogram (lanes 5–8). Although the fluorogram is somewhat underexposed, only two membrane proteins, the broad band 3 at ~97 kDa and a narrow 28 kDa band, were the primary photolabeling targets for the tritiated ligand (see also Fig. 2). Radioactivity measurements, as determined by gel slice quantitation, confirmed the photolabeling patterns as seen using gel fluorography. Coomassie does not stain the 28 kDa component, and detects band 3 only weakly (lanes 2–4), a well-known characteristic of glycosylated membrane proteins. The silver stain reveals a 28 kDa peptide in all three blood samples (lanes 10–12), aligning to the lower band in the fluorogram.

3.2. Photolabeling with [^{3}H]p-AzBPhz: effect of temperature

As expected, changes in temperature affected the photolabeling process (see Table 1). Alteration of the temperature appeared to primarily influence labeling of the 28 kDa protein with less effect on the anion transporter. If cells were initially cooled to 3°C and then incubated in the cold with [^{3}H]*p*-AzBPhz and

flashed cold (C/C/C), 35% less band 3 binding but 59% less incorporation into the 28 kDa peptide was observed than when all steps were carried out at 37°C (37/37/37). Two other temperature manipulations involved ambient (RT ≈ 24°C) cells incubated with the azide at RT, then cooling to 3°C and flashing cold (RT/RT/C); and, RT cells incubated with *p*-AzBPhz at RT and flashed at RT (RT/RT/RT). Although no difference in the relative labeling of the membrane proteins could be detected at either RT or 37°C, there was a slight increase in the total bound ligand when labeling was carried out at 37°C.

In some experiments, the azide was added to RBCs and incubated at RT in subdued light as described. Cells were then chilled to 3°C and washed twice with cold GGBS to remove free ligand. The cold mixture was then photolyzed as usual. This experimental variation produced a somewhat less intense, but otherwise identical labeling pattern on fluorograms (data not shown), as when the cold wash steps were not included. This finding indicates that labeling of the two target proteins was not due to promiscuous targeting by photoactivated *unbound* ligand.

3.3. Ligand dose-response and inhibition of protein labeling

The fluorogram in Fig. 2 represents the photolabeling pattern under three conditions, identical except for azide level, analyzed on a single gel. The tritiated *p*-AzBPhz was used over the range 0.2 and 2 μM, corresponding to $\sim 3 \times 10^5$ to 3×10^6 molecules *added* per cell (or ghost), the same level that causes the cellular changes described in our earlier experiments [6,7]. The anion transporter has previously been shown to be half-maximally inhibited when $< 0.5 \times 10^6$ molecules of *p*-AzBPhz are bound per cell with binding remaining linear to nearly 5 μM [15]. The effect of DIDS and *p*-CMBS on photolabeling is also shown. At a stoichiometry of less than 1

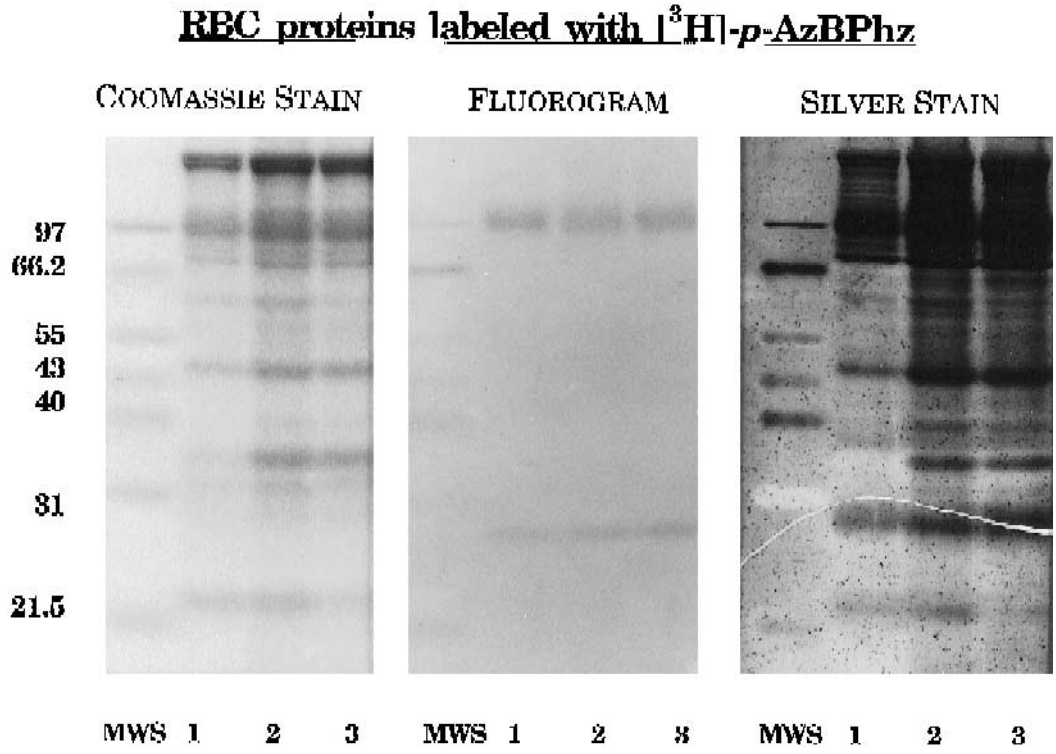

Fig. 1. Labeled red cell proteins separated by polyacrylamide gel electrophoresis. Each panel of the composite contains the same molecular weight standards (MWS) and photolabeled blood from 3 different individuals (1, 2, 3). Shown are Coomassie stained gel, fluorogram, and silver stained gel. The fluorogram shows the differential photolabeling of band 3 and a 28 kDa peptide with [^{3}H] *p*-AzBPhz at 1 μM. The 28 kDa protein is not readily visible with Coomassie stain, but is easily detected with the silver stain.

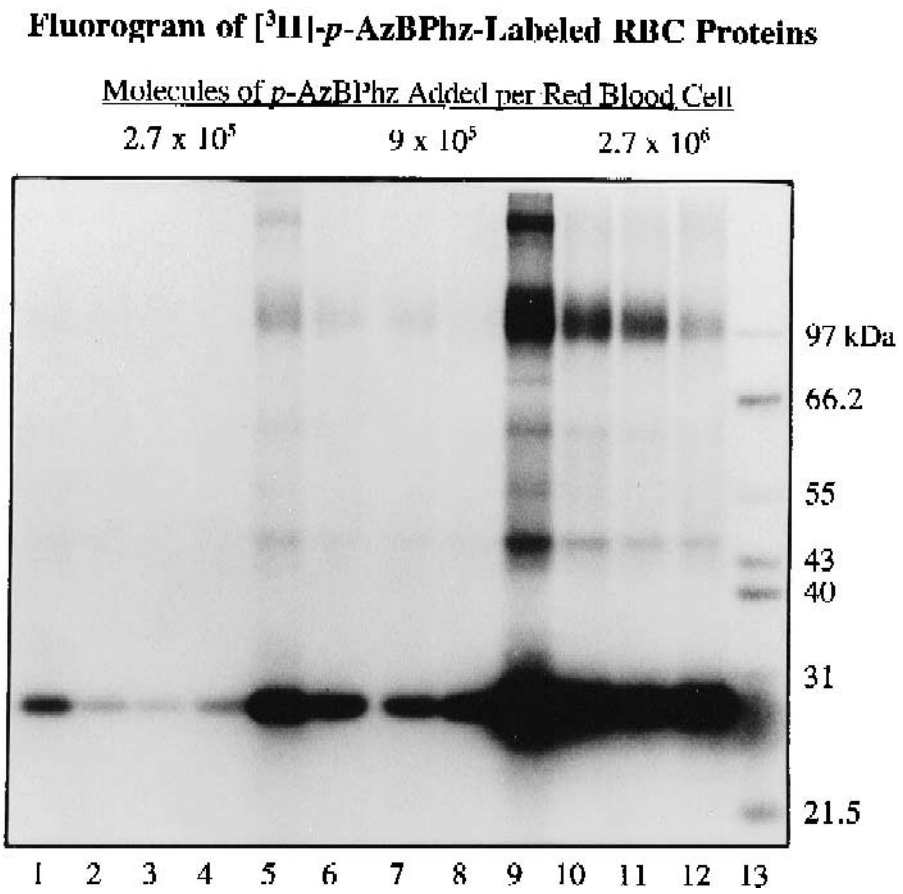

Fig. 2. Fluorogram showing the pattern of radioactively labeled protein bands in a series of dose-response conditions with three levels of ligand molecules *added* per cell or ghost. The leaky ghosts (lanes 1, 5, and 9) indicate that if allowed to, the azide will enter the cell and label internal proteins. The control red cell lanes (2, 6, and 10) show the differential labeling that occurs. The effects of 200 μM *p*-CMBS and 20 μM DIDS (lanes 3, 7, 11, and 4, 8, 12, respectively) are also shown; DIDS slightly inhibits band 3 binding and *p*-CMBS inhibits binding to the 28 kDa protein. See text for further discussion.

Table 1
Temperature dependent [^{3}H] *p*-AzBPhz incorporation into RBC membrane proteins

	C/C/C	RT/RT/C	RT/RT/RT	37/37/37
% incorporation ($n = 7$)	2.7 ±1.1 (A)	3.0 ±0.8 (A)	4.3 ±0.8 (B)	5.2 ±0.9 (B)
Band 3 density ($n = 10$)	1.01 ± 0.23 (A)	1.37 ± 0.25 (B)	1.45 ± 0.29 (B)	1.55 ± 0.36 (B)
28 kDa density ($n = 10$)	0.38 ± 0.18 (A)	0.55 ± 0.27 (AB)	0.76 ± 0.23 (BC)	0.93 ± 0.25 (C)
Band 3/28 kDa ratio	2.66	2.49	1.91	1.67

2 min flash at 1 mW/cm^2 using a 5% RBC suspension incorporated about 3–5% of the total 1 μM of ligand added. Percent incorporation was determined directly from scintillation counts while the proportional, arbitrary density values of both proteins were determined densitometrically from the PAG fluorograms. The conditions were: (C/C/C), cells and ligand were incubated and photolyzed in the cold (3°C); (RT/RT/C), cells and ligand were incubated at room temperature (24°C), then cooled and flashed at 3°C; (RT/RT/RT); all steps at 24°C; (37/37/37), all steps at 37°C; see text for details. Increasing temperature primarily influenced 28 kDa band labeling and had less effect on band 3. Values listed are means ± S.D. ANOVA shows significance at $P \leq 0.001$ for all categories. Newman-Keuls' post-hoc test ($P \leq 0.01$) indicates differences as shown in parentheses with letter differences implying significance within categories.

azide per available band 3 moiety (assuming each red cell possesses 10^6 copies of the anion exchanger), only labeling of the 28 kDa peptide was detectable, more so in leaky ghosts than in intact cells. When the level of azide was increased 3 and 10 fold, band 3 became labeled. Whereas this preferential photolabeling of both band 3 and the 28 kDa peptide was consistently observed, blood from some individuals showed a preference for labeling of one or the other.

At the higher ligand concentrations, cytoplasmic proteins also were photolabeled, but only when ghosts were tested. When red cells are carefully isolated, they remain impermeable to the azide, but if allowed to penetrate, the activated agent readily labels internal proteins, especially α and β spectrin at ~220–250 kDa, residual hemoglobin, and perhaps actin at ~43 kDa, ankyrin at 215 kDa and bands 4.1 and 4.2 at 78 and 70 kDa. When intact cells were examined at the highest level of azide tested, the only other radioactivity appeared as a faint band at 55–60 kDa (the glucose transporter?) and a prominent unknown band at 45–47 kDa.

Fig. 2 also shows that DIDS at 20 μM partially inhibited tritium incorporation into band 3, whereas *p*-CMBS at 200 μM primarily blocked label incorporation into the 28 kDa peptide. The results of a more comprehensive inhibition study, in which photolabeling was conducted at a constant [^{3}H] *p*-AzBPhz level of 1 μM, is displayed in Fig. 3. Panel A shows the expected result of adding non-radioactive azide to the incubation; namely, that photolabel incorporation into both target proteins was reduced with the same IC_{50} of about 25 μM. Addition of DIDS produced a surprising result (Panel B). Band 3 labeling was blocked by ~10% with 2.5 μM DIDS, progressing to only 15–20%, maximally. However, increasing the DIDS level caused a progressive dose-dependent *enhancement* of label incorporation into the 28 kDa peptide.

Two agents commonly used as inhibitors of red

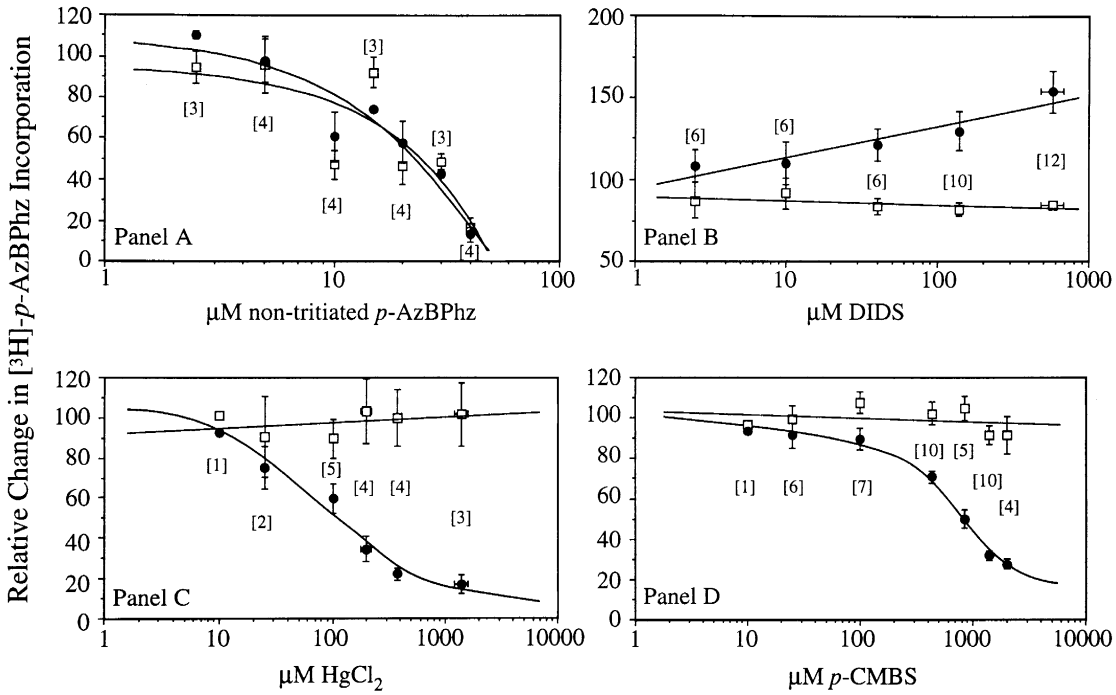

Fig. 3. Inhibition studies performed with [^{3}H] *p*-AzBPhz at 1 μM, plotted as change in photo-incorporation with arbitrary value of 100 to indicate the amount of bound azide without the addition of antagonist (band 3, open squares; 28 kDa peptide, closed circles). Panel A shows the results using nonradioactive *p*-AzBPhz with an IC_{50} of ~25 μM for both proteins. DIDS (panel B) showed limited band 3 labeling inhibition but with a progressive labeling enhancement of the 28 kDa band. Neither $HgCl_2$ (panel C) nor *p*-CMBS (panel D) had any effect on band 3 labeling but blocked labeling of the 28 kDa peptide with IC_{50} values of ~150 μM and ~0.9 mM, respectively. Data are represented as means ± S.E.M.; values in brackets indicate the number of observations for each point.

cell water flux include $HgCl_2$ and the more selective *p*-CMBS [9–11]. Neither compound had any apparent effect on band 3 labeling. Mercuric chloride (panel C) and *p*-CMBS (panel D) blocked labeling of the 28 kDa peptide with IC_{50}'s of about 150 μM and 0.9 mM, respectively. In control experiments, none of these inhibitors chemically modified the azide under the photolysis conditions, as verified by TLC of incubated samples.

3.4. Action of deglycosylation enzymes on the receptor proteins

The fluorogram displayed in Fig. 4 shows the results of deglycosylation experiments with the isolated, azide-photolabeled receptor proteins. PNGase F cleaved the band 3 oligosaccharides and reduced its MW_{app} by about 5 kDa. Occasionally, two minor peptides of about 64 and 50 kDa were observed; these were also shifted to higher R_f following treatment with PNGase F. The genesis of these lower M_r bands is unknown. However, Glyko quality control indicated that protease activity was not detectable. Also, smaller products were not observed for either the fetuin control or the 28 kDa peptide. Neither NANase II with *O*-glycosidase nor NANase III caused any apparent change to band 3.

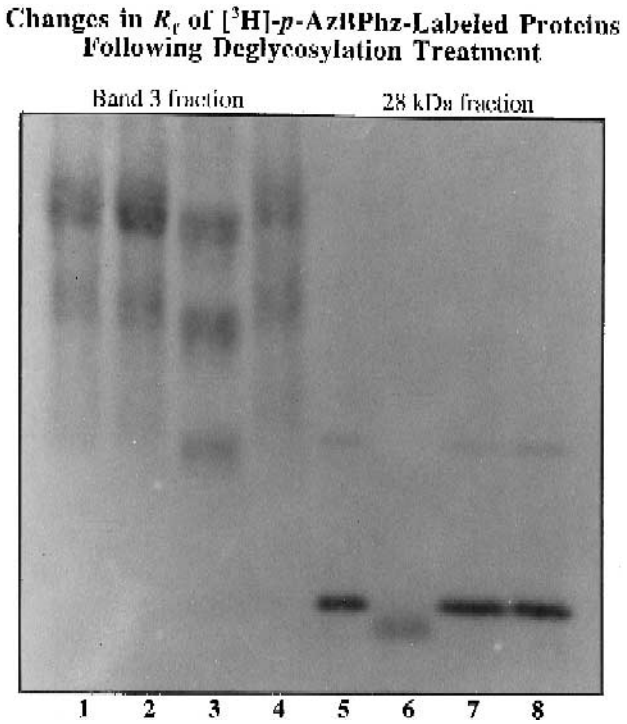

Fig. 4. Gel-purified, photolabeled proteins were treated with glycosidases to determine their glycoprotein character. Fluorograms show PAGE R_f changes following deglycosylation treatment. Treatment with NANase III had no effect on band 3 (lane 2), with respect to control (lane 1), but caused a shift in the 28 kDa peptide control M_r from 28.3 ± 0.7 kDa (lane 5) to 26.1 ± 0.4 (lane 6). Treatment with PNGase F merely deglycosylated band 3 ($\sim$ 5 kDa decrease in M_r from control, lane 1) with no effect on the 28 kDa peptide (lanes 3 and 7, respectively). *O*-glycosidase, in combination with NANase II (lanes 4 and 8), caused no apparent changes for any protein. See text for further discussion.

The radioactive 28 kDa peptide (28.3 ± 0.7 kDa) fraction, as isolated by our method (Fig. 4, lane 5), shows an unexpected band with a MW_{app} of 47 ± 1 kDa. This may represent a 5% aggregation of the receptor protein; it is not simply a contaminant of the 28 kDa isolate since the electroeluted gel was carefully sliced between the range of 26–31 kDa. No other proteins could be detected by silver staining. Treatment with NANase III caused an R_f shift to 26.1 ± 0.4 kDa of the major band (lane 6), suggesting the presence of a β2-3,6 or 8-linked *N*-acetylneuraminic acid; the faint 47 kDa band was also digested and shifted to 42.3 ± 0.6. Neither PNGase F (lane 7) nor treatment with *O*-glycosidase in combination with NANase II (lane 8) had any effect under our conditions. However, incubation with *O*-glycosidase followed by PNGase F treatment may have induced a slight (non-verifiable) R_f increase in the 28 kDa peptide (not shown). Identical pattern changes of the major radioactive bands were found when the native proteins in cell or ghost membranes were exposed to these enzymes.

4. Discussion

Interactions between the membrane and underlying cytoskeleton give the red cell its inherent characteristics of shape, stability, and elasticity – intrinsic features that are all altered by *p*-AzBPhz [6,7]. The present photolabeling experiments were conducted to identify the candidate receptor proteins through which the azide could affect these cell properties. The anion transporter and a 28 kDa peptide were selectively photolabeled in a dose-dependent manner under essentially the same conditions that we observed azide-

induced cell changes. We initially thought that the primary receptor was CHIP28 (AQP1) [16,17], based on its R_f and Coomassie staining-resistant characteristics on polyacrylamide gels, its resistance to PNGase F digestion [18], and the inhibition of azide labeling by small concentrations of the water channel blockers, $HgCl_2$ and *p*-CMBS. However, after discussing these results with Dr Michael L. Jennings, he performed immunoblotting that did not support this idea (personal communication). As stated here, Jennings also observed that upon re-electrophoresis of gel-purified 28 kDa protein, the appearance of a second higher M_r band at about 42 kDa (M_r based on colored standards, as opposed to our native protein standards) was seen, detectable with his monoclonal antibody against CHIP28. Upon treatment of his isolated protein with NANase III, no antibody-detectable shift in the 28 kDa band occurred, in contradistinction to our finding (Fig. 4, lane 3). However, anti-CHIP28 antibody did detect that the higher M_r band was shifted to a higher R_f, as we found with our photolabeled 47 kDa band. It therefore appears that the 28 kDa region of the SDS-PAGE gel contains at least two proteins; a CHIP28 antibody-detectable component and an azide-photolabeled peptide. It is likely that when this mixture is re-electrophoresed a partial heterodimerization of these two components occurs. These findings, in light of our previous work [6,7] and two recent reports on the lack of CHIP28 in human cells that have high capacity for water flux [19,20], suggest that isoforms of the water channel exist and that our photolabeling probe may have identified either an aquaporin that fails to react with anti-CHIP28 antibody or an aquaporin-modulating peptide.

Low concentrations of DIDS antagonized covalent incorporation into band 3, but its inhibitory effects were minimal, perhaps due (in part) to this agent's complex time-dependent interaction with band 3. However, DIDS had an additional unexpected action; as it blocked labeling of the anion exchanger, it caused a dose-dependent increase in photolabeling of the 28 kDa peptide. An obvious first explanation for this result is that by preventing the azide's interaction with band 3, more azide was made available for binding to the smaller peptide. However, this appears not to be consistent with the observation that at the lowest concentration of DIDS (2.5 μM), about 10% of band 3 labeling inhibition had already occurred, without promotion of 28 kDa labeling.

Another explanation, that the DIDS interaction with the anion transporter makes the 28 kDa protein more accessible to the azide, relates to the idea proposed by Solomon and his coworkers [21,22] who suggested that the same proteins that serve as receptors for our ligand (including band 4.5, the glucose transporter) are physically associated to facilitate an intermolecular interplay in the control of transport events in the cell. Whereas band 4.5 becomes photolabeled only at higher ligand doses, *p*-AzBPhz markedly inhibits this transporter [12,15]. The association of proteins in a transport complex could also explain why *p*-AzBPhz's photolabeling of the two target proteins is differentially affected by temperature (Table 1). The ratio of band 3 to 28 kDa peptide label incorporation at 3°C is nearly double that found in experiments conducted at $\geq$ RT. This indicates that at low temperatures, when the receptor proteins are likely to exist in a more tightly associated state, the 28 kDa binding site is less accessible for photolabeling. Alternatively, the temperature-dependent photolabeling differences that were observed with the two proteins may simply follow from their having different Arrhenius plot profiles.

Inhibition of 1 μM [^{3}H]*p*-AzBPhz protein labeling with non-radioactive azide gave an IC_{50} of about 25 μM. The results in which the cellular actions of the azide were examined indicated that the apparent K_d of the ligand was about 1–2 μM [12,15]. Based on this value, classical competitive inhibition theory predicts that at 1 μM radiolabeled ligand, the IC_{50} of the non-labeled azide should be about 2–3 μM. However, for this assumption to be valid, the receptor concentration must be very much lower than either K_d or K_i, and this condition does not exist in the present work. The high specific activity of the tritiated azide provided the opportunity to examine the ligand at approximately a 1 : 1 stoichiometry between molecules of added azide and the combined total number of band 3 and 28 kDa peptide molecules in the cell suspension. With a receptor-to-ligand ratio so small, binding is likely to be stoichiometric, appear 'pseudo-irreversible', and require greater amounts of antagonist.

Neither of the mercurials had any apparent affect on band 3 photolabeling, but both blocked label

incorporation of the 28 kDa protein. The IC_{50} values of about 150 μM and 0.9 mM for mercuric chloride and *p*-CMBS respectively (Fig. 3), agrees with the observation by others that water transport inhibition is more sensitive to $HgCl_2$ than *p*-CMBS [23,24].

The single asparagine (*N*)-linked oligosaccharide chain on band 3 [25], was not the exofacial target site for the photo-incorporation of the azide. When the photolabeled membranes or the isolated, labeled protein was treated with PNGase F, (which specifically cleaves asparagine-linked mannose residues), the R_f of a sharper stained band was increased and its fluorography signal was intensified. This result is compatible with that found by Mueller [26] who observed a similar effect on Coomassie stained gels following endo-β-galactosidase exposure.

Following enzymatic treatment with NANase III, an enzyme that releases β2-3,6,8-linked *N*-acetylneuraminic acid, the mobility of our 28 kDa protein was increased. Since combined assays in the presence of NANase II, which splits β2-3,6-linked *N*-acetylneuraminic acid, did not result in any apparent alteration in R_f, it appears that sialic acid is linked to this receptor protein in a β2-8 linkage. What sugar serves as the attachment moiety is unknown. The oligosaccharide moieties on this peptide also were not the target sites for the photoactivated ligand. The glycophorins are linked through an *O*-glycosylation site [27] while AQP1 is glycosylated through an *N*-linked oligosaccharide chain [28].

The results presented here are consistent with our earlier hypothesis that the improved rheology and small increase in water content in the red blood cell occurs through a stoichiometric interaction of *p*-AzBPhz with the anion exchanger and a 28 kDa peptide that is similar or affiliated with the RBC water channel. It appears that the ligand induces a band 3 conformational change, and this trans-membrane signal mediates an increase in cytoskeletal entropy whereby the underlying spectrin scaffolding becomes more flexible. This view is consistent with the observations by others that an exofacial band 3-DIDS interaction can lead to changes in the cytoplasmic domain [29,30]. Water influx, proportional to azide dose, is associated with these events. They may be (partially) mediated by band 3 and the 28 kDa peptide through a transport-complex-modulated aquaporin-type channel. Cell shape changes occur due to an easily reversible rearrangement of the cytoskeleton, flexibility increases, and the cell maximally swells 10% to a new steady-state [6,7,15], effects especially pronounced in cells of individuals affected with sickle cell disease [7].

While the driving force for this water flux has not been elucidated, we have previously proposed an explanation for the ligand-induced changes in the red cell's osmotic transitions [6,7]. Recent work by Haines [31] suggests that an increase in phospholipid chain motion in the lipid membrane facilitates water movement through the bilayer and that agents which decrease lateral diffusion reduce water flux. The effects on the cell at low μM levels of *p*-AzBPhz are not likely to be the result of this lipid insertion mechanism (which was also proposed by Deuticke [32] for phloretin, the aglycone of our ligand) since we found insignificant photo-incorporation into membrane lipids at these concentrations. Furthermore, it has been demonstrated that the azide does not disturb the motion of the bulk lipid [33].

References

[1] S.-C. Liu, L.H. Derick, Semin. Hematol. 29 (1992) 231–243.
[2] E.J. Luna, A.L. Hitt, Science 258 (1992) 955–963.
[3] D.M. Gilligan, V. Bennett, Semin. Hematol. 30 (1993) 74–83.
[4] N.J. Hemming, D.J. Anstee, M.A. Staricoff, M.J. Tanner, N. Mohandas, J. Biol. Chem. 270 (1995) 5360–5366.
[5] D.J. Anstee, N.J. Hemming, M.J. Tanner, Immunol. Invest. 24 (1995) 187–198.
[6] M.E. Blank, D.M. Hoefner, D.F. Diedrich, Biochim. Biophys. Acta 1192 (1994) 223–233.
[7] D.M. Hoefner, M.E. Blank, B.M. Davis, D.F. Diedrich, J. Membrane Biol. 141 (1994) 91–100.
[8] U.K. Laemmli, Nature 227 (1970) 680–685.
[9] G.M. Preston, T.P. Carroll, W.B. Guggino, P. Agre, Science 256 (1992) 385–387.
[10] R.I. Macey, D.M. Karan, J. Membrane Biol. 134 (1993) 241–250.
[11] G. Benga, Prog. Biophys. Mol. Biol. 51 (1988) 193–245.
[12] D.F. Diedrich, Methods Enzymol. 191 (1990) 755–780.
[13] T.B. Shea, BioTechniques 16 (1994) 1126–1128.
[14] A.S. Bhown, J.E. Mole, F. Hunter, J.C. Bennett, Anal. Biochem. 103 (1980) 184–190.
[15] M.E. Blank, D.F. Diedrich, Biorheology 27 (1990) 345–355.
[16] P. Agre, D. Brown, S. Nielsen, Curr. Opin. Cell Biol. 7 (1995) 472–483.
[17] A.S. Verkman, A.N. Van Hoek, T. Ma, A. Frigeri, W.R. Skach, A. Mitra, B.K. Tamarappoo, J. Farinas, Am. J. Physiol. 270 (1996) C12–C30.

[18] A.N. Van Hoek, M.C. Wiener, J.-M. Verbavatz, D. Brown, P.H. Lipniunas, R.R. Townsend, A.S. Verkman, Biochemistry 34 (1995) 2212–2219.
[19] C. Liu, D. Gao, G.M. Preston, L.E. McGann, C.T. Benson, E.S. Critser, J.K. Critser, Biol. Reprod. 52 (1995) 913–919.
[20] G.M. Preston, B.L. Smith, M.L. Zeidel, J.J. Moulds, P. Agre, Science 265 (1994) 1585–1587.
[21] G. Kifor, M.R. Toon, A. Janoshazi, A.K. Solomon, J. Membrane Biol. 134 (1993) 169–179.
[22] M.R. Toon, A.K. Solomon, Biochim. Biophys. Acta 1193 (1994) 276–286.
[23] M.L. Zeidel, A. Albalak, E. Grossman, A. Carruthers, Biochemistry 31 (1992) 589–596.
[24] M.L. Zeidel, S.V. Ambudkar, B.L. Smith, P. Agre, Biochemistry 31 (1992) 7436–7440.
[25] M.J.A. Tanner, P.G. Martin, S. High, Biochem. J. 256 (1988) 703–712.
[26] T.J. Mueller, Y.-T. Li, M. Morrison, J. Biol. Chem. 254 (1979) 8103–8106.
[27] J.A. Chasis, N. Mohandas, Blood 80 (1992) 1869–1879.
[28] B.M. Denker, B.L. Smith, F.P. Kuhajda, P. Agre, J. Biol. Chem. 263 (1988) 15634–15642.
[29] L. Hsu, M. Morrison, Arch. Biochem. Biophys. 227 (1983) 31–38.
[30] J.M. Salhany, K.A. Cordes, E.D. Gaines, Biochemistry 19 (1980) 1447–1454.
[31] T.H. Haines, FEBS Lett. 346 (1994) 115–122.
[32] B. Deuticke, Biochim. Biophys. Acta 163 (1968) 494–500.
[33] J.W. Wyse, M.E. Blank, C.L. Maynard, D.F. Diedrich, D.A. Butterfield, Biochim. Biophys. Acta 979 (1989) 127–131.